DOI: 10.13009/EUCASS2017-281

Numerical simulation of flow over space vehicle in Martian atmosphere

I. V. Egorov and M.A. Pugach***
**Central Aerohydrodynamic Institute*
1 Zhukovsky street, Zhukovsky, Moscow region, Russia
***Moscow Institute of Physics and Technology*
9 Institutsky pereulok, Dolgoprudny, Moscow region, Russia

Abstract

Method of simulation of three-dimensional flow over real bodies based on numerical solution of Navier-Stokes equations with nonequilibrium physical-chemical processes in Martian atmosphere. The method is based on implicit monotone approximation scheme and modified Newton-Raphson technique for solution of nonlinear difference equations. As an example, three-dimensional hypersonic flow over a segmental-conical body similar to the Martian space vehicle "ExoMars" is studied. For two trajectory points in Martian atmosphere and two angles of attack of free stream high-temperature gas flow in the vicinity of space vehicle is analyzed. Influence of catalytic properties of descent module surface on aerodynamic heating is shown.

1. Introduction

Descent space vehicles are key elements of interplanetary space investigations. Such vehicles are very significant, since they allow delivering research equipment to other planets. Nowadays investigations of Mars planet are carried out. Space vehicles, developed for descent on Mars, are ordinarily have segmental-conical shape, which consists of front part (spherical shape, blunted circular cone shape with large half-angle) and converging conic afterbody with spherical or butt end. Such shape allows increasing drag coefficient and thus providing stability of a vehicle during the flight along trajectory, so that conditions of ballistic descent are satisfied. However, vehicle should be oriented at angle of attack , relative to free stream, in order to achieve more effective aerodynamic deceleration. As result, flow over the vehicle is essentially non-symmetric, and three-dimensional effects like flow separation on the leeward side, reversed flow in base region, evolution and structure of separation zone play important part.

Furthermore, descent vehicles enter Earth and Martian atmospheres at high velocities (M = 30), and this leads to significant influence of physical-chemical processes on flow and heat transfer in the vicinity of the vehicle [1]. Martian atmosphere consists mainly of carbon dioxide (98 %) and 100 times more rarefied, than Earth atmosphere, nevertheless, high descent velocities lead to strong aerodynamic heating of vehicle surface.

Currently mathematical simulation for aerodynamic characteristics of segmental-conical bodies is actively developed, which allows obtaining detailed flow pattern. Experimental studies of this field are rather, since they can't simulate real flight conditions.

One of main goals of this work is testing of developed method and programs, using calculation of flow over segmental-conical body. Previously this method is employed to direct numerical simulation of laminar-turbulent transition on basis of Navier-Stokes equations and supersonic flow over segmental-conical body on basis of Reynolds equations with two-parameter differential turbulence model [2]. In this work three-dimensional hypersonic flow over segmental-conical body, similar to Martian space vehicle "ExoMars", is considered. Simulation is based on numerical simulation of Navier-Stokes equations jointly with nonequilibrium physical-chemical processes. Solution is carried out using original software package HSFlow with effective parallel algorithm for supercomputers.

2. The problem statement

Within the framework of continuum mechanics motion of gas medium in general case is described by three-dimensional Navier-Stokes equations for chemically nonequilibrium gas mixture. These equations express laws of

DOI: 10.13009/EUCASS2017-281

mass, moment and energy conservation and can be written in conservative form in arbitrary curvilinear coordinate system ξ, η, ζ (where $x = x(\xi,\eta,\zeta)$, $y = y(\xi,\eta,\zeta)$, $z = z(\xi,\eta,\zeta)$ –Cartesian coordinates)

$$\frac{\partial \mathbf{Q}}{\partial t} + \frac{\partial \mathbf{E}}{\partial \xi} + \frac{\partial \mathbf{G}}{\partial \eta} + \frac{\partial \mathbf{F}}{\partial \zeta} = \mathbf{S}. \qquad (1)$$

Here **Q** – vector of conservative dependent variables, **E**, **G**, **F** — flux vectors in curvilinear coordinate system, **S** — source vector. Vectors **Q**, **E**, **G**, **F, S** are related to corresponding vectors $\mathbf{Q}_c$, $\mathbf{E}_c$, $\mathbf{G}_c$, $\mathbf{F}_c$, $\mathbf{S}_c$ in Cartesian coordinate system by formulas

$$\mathbf{Q}=J\mathbf{Q}_c, \quad \mathbf{S}=J\mathbf{S}_c, \quad \mathbf{E} = J(\mathbf{E}_c \frac{\partial \xi}{\partial x} + \mathbf{G}_c \frac{\partial \xi}{\partial y} + \mathbf{F}_c \frac{\partial \xi}{\partial z}),$$

$$\mathbf{G} = J(\mathbf{E}_c \frac{\partial \eta}{\partial x} + \mathbf{G}_c \frac{\partial \eta}{\partial y} + \mathbf{F}_c \frac{\partial \eta}{\partial z}), \quad \mathbf{F} = J(\mathbf{E}_c \frac{\partial \zeta}{\partial x} + \mathbf{G}_c \frac{\partial \zeta}{\partial y} + \mathbf{F}_c \frac{\partial \zeta}{\partial z})$$

where $J = \partial(x, y, z)/\partial(\xi, \eta, \zeta)$ – transformation Jacobian.

Curvilinear coordinate system (ξ, η, ζ) is used for discretization on uniform grid: arbitrary computational grid in Cartesian coordinate system is mapped on uniform grid in curvilinear coordinate system.
Cartesian components of flux vectors $\mathbf{Q}_c$, $\mathbf{E}_c$, $\mathbf{G}_c$, $\mathbf{F}_c$, $\mathbf{S}_c$ for three-dimensional Navier-Stokes equations are as follows:

$$\mathbf{Q}_c = \begin{Vmatrix} \rho_i \\ \rho u \\ \rho v \\ \rho w \\ \rho e \end{Vmatrix}, \ \mathbf{E}_c = \begin{Vmatrix} \rho_i u + I_x^i \\ \rho u^2 + p + \tau_{xx} \\ \rho uv + \tau_{xy} \\ \rho uw + \tau_{xz} \\ \rho uH + q_x \end{Vmatrix}, \ \mathbf{G}_c = \begin{Vmatrix} \rho_i v + I_y^i \\ \rho uv + \tau_{yx} \\ \rho v^2 + p + \tau_{yy} \\ \rho vw + \tau_{yz} \\ \rho vH + q_y \end{Vmatrix}, \ \mathbf{F}_c = \begin{Vmatrix} \rho_i w + I_z^i \\ \rho uw + \tau_{zx} \\ \rho vw + \tau_{zy} \\ \rho w^2 + p + \tau_{zz} \\ \rho wH + q_y \end{Vmatrix}, \ \mathbf{S}_c = \begin{Vmatrix} \omega_i \\ 0 \\ 0 \\ 0 \\ 0 \end{Vmatrix},$$

where u, v, w — Cartesian components of velocity vector **V**, p - pressure, ρ — total density of gas mixture, ρ_i — density of i-th gas mixture component (i = 1, …, K); K — the number of gas mixture species, $e = h - \frac{p}{\rho} + \frac{1}{2}\left(u^2 + v^2 + w^2\right)$ — total energy per unit volume, $H = h + \left(u^2 + v^2 + w^2\right)/2$ — total enthalpy, $h = \sum_{i=1}^{K} h_i C_i$ — static enthalpy of gas mixture, C_i, ω_i, h_i — mass fractions, production rates, static enthalpies of gas mixture species correspondingly, $\boldsymbol{\tau}$ - symmetric viscous stress tensor, related to strain velocity tensor **s** by linear dependence $\boldsymbol{\tau} = -\mu\mathbf{s}$.

Components of strain velocity tensor **s** for compressible gas are as follows:

$$s_{xx} = 2\frac{\partial u}{\partial x} - \frac{2}{3}\mathrm{div}\mathbf{V}, \ s_{yy} = 2\frac{\partial v}{\partial y} - \frac{2}{3}\mathrm{div}\mathbf{V}, \ s_{zz} = 2\frac{\partial w}{\partial z} - \frac{2}{3}\mathrm{div}\mathbf{V},$$

$$s_{xy} = s_{yx} = \frac{\partial u}{\partial y} + \frac{\partial v}{\partial x}, \ s_{xz} = s_{zx} = \frac{\partial u}{\partial z} + \frac{\partial w}{\partial x}, \ s_{yz} = s_{zy} = \frac{\partial v}{\partial z} + \frac{\partial w}{\partial y}.$$

Heat flux vector **q** is determined by following expression:

$$\mathbf{q} = -\lambda \,\mathrm{grad}\left(T\right) + \boldsymbol{\tau}\mathbf{V} + \sum_{i=1}^{K} h_i \mathbf{I}^i \ .$$

Here $\mathbf{I}^i$ — diffusive flux vector of i-th mixture species, which in this work is determined on basis of Fick law with approximation of binary diffusion model:

$$\mathbf{I}^i = -\rho D_i \,\mathrm{grad}\left(C_i\right),$$

DOI: 10.13009/EUCASS2017-281

where μ, λ and D_i — coefficients of molecular viscosity, thermal conductivity and diffusion.

For calculations of viscosity coefficient dependency $\frac{\mu}{\mu_\infty} = \left(\frac{T}{T_\infty}\right)^\omega$ is used (in this work $\omega = 0.731$), thermal conductivity coefficient is determined from expression for Prandtl number $\mathrm{Pr} = \frac{\mu c_p}{\lambda} = 0.7$, and diffusion coefficients D_i — from expression for Schmidt number $\mathrm{Sc}_i = \frac{\mu}{\rho D_i} = 0.5$ for all species of gas mixture. Index "∞" corresponds to free stream values.
Set of equations (1) is closed by algebraic equations: equation of state for gas mixture

$$p = \frac{\rho R T}{M},\ M = \left(\sum_{i=1}^{K} \frac{C_i}{M_i}\right)^{-1} \tag{2}$$

where R – universal gas, M — molar weight of gas mixture; and also by relationships for sum of mass fractions and diffusive fluxes of gas mixture components:

$$\sum_{i=1}^{K} C_i = 1,\quad \sum_{i=1}^{K} \mathbf{I}^i = 0$$

In this work 8 - species gas model, representing Martian atmosphere (K=8: O, N, NO, O_2, N_2, CO_2, CO, C), is considered. Species generation rates are determined on basis of mass action law, and chemical reaction rate constants are calculated according to Arrhenius equation:

$$k_{f(b),i} = A_{f(b),\mathrm{i}} T^{B_{f(b),i}} \exp\left(-\frac{D_{f(b),i}}{T}\right),$$

where $k_{f(b),i}$ — forward (*f*) and back (*b*) chemical reaction rate constants, $A_{f(b),i}$, $B_{f(b),i}$, $D_{f(b),i}$ – approximation coefficients, T – temperature of molecule translational motion, i – number of chemical reactions. Forward and back chemical reaction rate constants are taken from [3].
The following 12 dissociation and exchange reactions are taking into account in simulation of chemical processes in Martian atmosphere:

$N_2 + M \leftrightarrow N + N + M$
$O_2 + M \leftrightarrow O + O + M$
$CO + M \leftrightarrow C + O + M$
$NO + M \leftrightarrow N + O + M$
$CO_2 + M \leftrightarrow CO + O + M$
$NO + O \leftrightarrow N + O_2$
$N_2 + O \leftrightarrow NO + N$
$CO + O \leftrightarrow O_2 + C$
$CO_2 + O \leftrightarrow O_2 + CO$
$CO + N \leftrightarrow NO + C$
$CO + CO \leftrightarrow CO_2 + C$
$NO + CO \leftrightarrow CO_2 + N$

Here M – catalytic particle, which can be any of species in the mixture.
Static enthalpy of gas mixture species is given by following formula

$$h_i = \frac{5}{2}\frac{RT}{M_i} + e_i^r(T) + e_i^v(T) + h_i^0,$$

DOI: 10.13009/EUCASS2017-281

Where $e_i^r(T)$ - excitation energy of rotational degrees of freedom, equal to $e_i^r(T) = \dfrac{RT}{M_i}$ for diatomic molecule and $e_i^r(T) = \dfrac{3}{2}\dfrac{RT}{M_i}$ for triatomic molecule CO_2; $e_i^v(T)$ - excitation energy of vibrational degrees of freedom, equal to $e_i^v(T) = \dfrac{RT_{vi}}{M_i}\dfrac{1}{e^{\frac{T_{vi}}{T}} - 1}$ for diatomic molecule and $e_i^v(T) = \sum_{k=1}^{3}\dfrac{RT_{vi,k}}{M_i}\dfrac{1}{e^{\frac{T_{vi,k}}{T}} - 1}$ for triatomic molecule CO_2; h_i^0 - formation enthalpy of gas mixture component. Values of vibrational temperatures and formation enthalpies, used in this work, are given in Table 1.

Table 1: Vibrational temperatures and formation enthalpies

Chemical species	Vibrational temperature T_{vi}, K	Formation enthalpy h_i^0, J × mole/kg
O	0.0	15.6×10^6
N	0.0	33.9×10^6
NO	2791.0	3.02×10^6
O_2	2256.0	0.0
N_2	3354.0	0.0
CO_2	960.0 1190.0 3380.0	-8.37×10^6
CO	3122.0	-4.06×10^6
C	0.0	59×10^6

Calculations are carried out for laminar flow. On the outer boundary of the computational domain either Dirichlet (on the front part) or extrapolation boundary conditions are set. Free stream mass fractions are similar to those in Martian atmosphere: $C_{CO_2} = 0.97$, $C_{N_2} = 0.03$, for other mixture mass fractions are equal to zero.

On the solid boundary of computational domain non-slippery boundary conditions ($u = 0, v = 0, w = 0$), conditions for heat flux and species mass fractions are set. On the assumption of low heat-conducting non-ablative heat shielding convective heat flux dissipates because of radiation, the following equation is valid:

$$q^*{}_w^n = \varepsilon\sigma^*\left(T_w^{*4} - T_\infty^{*4}\right),$$

where $q^*{}_w^n$ – projection of heat flux on the normal to the body surface, ε – emissivity of the body surface, value of which is taken to be equal to 0.9, σ^* – Stefan-Boltzmann constant. Dimensional quantities are marked by superscript "*".

For mass fractions of gas species on the surface following conditions are set:

— catalytic surface with respect to atomic oxygen and nitrogen

$$\left.\frac{\partial C_{NO}}{\partial n}\right|_w = \left.\frac{\partial C_{CO_2}}{\partial n}\right|_w = \left.\frac{\partial C_{CO}}{\partial n}\right|_w = 0,\ C_O\big|_w = C_N\big|_w = 0\ ,$$

— and absolutely non-catalytic surface

$$\left.\frac{\partial C_O}{\partial n}\right|_w = \left.\frac{\partial C_N}{\partial n}\right|_w = \left.\frac{\partial C_{NO}}{\partial n}\right|_w = \left.\frac{\partial C_{CO_2}}{\partial n}\right|_w = \left.\frac{\partial C_{CO}}{\partial n}\right|_w = 0\ .$$

On the boundary of computational domain, coinciding with symmetry plane $y = 0$, symmetry boundary conditions are set. On the degenerate surfaces, obtained as a result of symmetry axis rotation, extrapolation of dependent variables is set.

DOI: 10.13009/EUCASS2017-281

Uniform free stream is used as initial conditions with subsequent development of flow field during solution of unsteady problem. Time step is gradually increased for as far as flow field is formed.

2.1 Approximation of differential equations

Formulated initial-boundary problem is solved numerically on basis of finite volume method. Once applied to Navier-Stokes equations (1), it gives difference conservation laws

$$\frac{\mathbf{Q}^{n+1}_{i,j,k}-\mathbf{Q}^{n}_{i,j,k}}{\Delta t}+\frac{\mathbf{E}^{n+1}_{i+\frac{1}{2},j,k}-\mathbf{E}^{n+1}_{i-\frac{1}{2},j,k}}{h_\xi}+\frac{\mathbf{G}^{n+1}_{i,j+\frac{1}{2},k}-\mathbf{G}^{n+1}_{i,j-\frac{1}{2},k}}{h_\eta}+\frac{\mathbf{F}^{n+1}_{i,j,k+\frac{1}{2}}-\mathbf{F}^{n+1}_{i,j,k-\frac{1}{2}}}{h_\zeta}=S^{n+1}_{i,j,k}$$

where n – time layer number; Δt– time step; i, j, k and h_ξ, h_η, h_ζ — node numbers and steps for coordinates ξ, η, ζ correspondingly.

For approximation of convective component of flux vectors **E**, **G** and **F** at half-integer nodes Godunov type monotone scheme [4, 5] and approximate Roe method [6] for solution of Riemann problem are used. Formulas for **E** and **G**, **F** are similar, so below only **E** flux vector is considered. For **E** flux vector:

$$\mathbf{E}_{i+\frac{1}{2}}=\frac{1}{2}\Big[\mathbf{E}(\mathbf{Q_L})+\mathbf{E}(\mathbf{Q_R})-\mathbf{R}(\mathbf{Q_{LR}})\mathbf{\Phi}(\phi(\lambda_i))\mathbf{R}(\mathbf{Q_{LR}})^{-1}\left(\mathbf{Q_R}-\mathbf{Q_L}\right)\Big]$$

Where $\mathbf{\Phi}(\varphi(\lambda_i))$ — diagonal matrix, elements of which are $\phi(\lambda_i)$, and λ_i — eigenvalues of operator $\mathbf{A}=\partial\mathbf{E}/\partial\mathbf{Q}$. $\mathbf{R}_{LR}=\mathbf{R}(\mathbf{Q}_{LR})$ — matrix, columns of which are eigenvectors of operator **A**. $\mathbf{\Phi}(\phi(\lambda_i))$, $\mathbf{R}_{LR}$, $\mathbf{R}_{LR}^{-1}$ are determined by values of dependent variables

$$u_{\mathbf{LR}}=\frac{u_{\mathbf{L}}\sqrt{\rho_{\mathbf{L}}}+u_{\mathbf{R}}\sqrt{\rho_{\mathbf{R}}}}{\sqrt{\rho_{\mathbf{L}}}+\sqrt{\rho_{\mathbf{R}}}},\quad v_{\mathbf{LR}}=\frac{v_{\mathbf{L}}\sqrt{\rho_{\mathbf{L}}}+v_{\mathbf{R}}\sqrt{\rho_{\mathbf{R}}}}{\sqrt{\rho_{\mathbf{L}}}+\sqrt{\rho_{\mathbf{R}}}},\quad w_{\mathbf{LR}}=\frac{w_{\mathbf{L}}\sqrt{\rho_{\mathbf{L}}}+w_{\mathbf{R}}\sqrt{\rho_{\mathbf{R}}}}{\sqrt{\rho_{\mathbf{L}}}+\sqrt{\rho_{\mathbf{R}}}},$$

$$a_{\mathbf{LR}}=\frac{a_{\mathbf{L}}\sqrt{\rho_{\mathbf{L}}}+a_{\mathbf{R}}\sqrt{\rho_{\mathbf{R}}}}{\sqrt{\rho_{\mathbf{L}}}+\sqrt{\rho_{\mathbf{R}}}}$$

where c — local value of sound speed.

Solution of Riemann problem for chemically non-equilibrium gas mixture is reduced to solution of nonlinear system of algebraic equations. Approximate method of solution of this problem is its splitting using generalized coordinates and representation of some averaged state of corresponding Jacobian matrix $\mathbf{A}$ (e.g., $\mathbf{A}=\partial\mathbf{E}/\partial\mathbf{Q}$ for ξ direction, here $\mathbf{E}$ is a convective component of the corresponding flux) in diagonal form : $\mathbf{A}=\mathbf{R}\Lambda\mathbf{R}^{-1}$, where Λ – diagonal matrix, elements of which are eigenvalues of the matrix $\mathbf{A}$.

For operators $\partial\mathbf{G}/\partial\mathbf{Q}$ and $\partial\mathbf{F}/\partial\mathbf{Q}$ representation of eigenvalues and eigenvectors is carried out using the same formulas with replacement of ξ with η and ξ with ζ correspondingly.

A function $\phi(\lambda_i)$, providing entropy condition for physically correct choice of numerical solution, has the following form:

$$\phi(\lambda)=\begin{cases}|\lambda|, & |\lambda|>\varepsilon\\ \dfrac{\lambda^2+\varepsilon^2}{2\varepsilon}, & |\lambda|\le\varepsilon\end{cases}$$

where ε – dissipation parameter of numerical scheme.

In order to increase approximation order (to second) for interpolation of dependent variables on the boundary of elementary cell, minimal derivatives principle (MUSCL) [7-9] is used

$$\mathbf{Q_L}=\mathbf{Q}_i+\frac{1}{2}m\left(\mathbf{Q}_i-\mathbf{Q}_{i-1},\mathbf{Q}_{i+1}-\mathbf{Q}_i\right),\quad \mathbf{Q_R}=\mathbf{Q}_{i+1}-\frac{1}{2}m\left(\mathbf{Q}_{i+1}-\mathbf{Q}_i,\mathbf{Q}_{i+2}-\mathbf{Q}_{i+1}\right),$$

and function $m(a,b)$ is

$$m(a,b)=\operatorname{minmod}(a,b)=\begin{cases}a, & ab>0,\ |a|<|b|\\ b, & ab>0,\ |a|>|b|\\ 0, & ab\le 0\end{cases}$$

DOI: 10.13009/EUCASS2017-281

For approximation of diffusive components of flux vectors **E**, **G** and **F** central-difference numerical scheme of second approximation order is used. For derivative calculation the following formulas are used

$$\left.\frac{\partial \mathbf{U}}{\partial \xi}\right|_{i+\frac{1}{2},j,k} = \frac{1}{h_\xi}\left(\mathbf{U}_{i+1,j,k} - \mathbf{U}_{i,j,k}\right),$$

$$\left.\frac{\partial \mathbf{U}}{\partial \eta}\right|_{i+\frac{1}{2},j,k} = \frac{1}{4h_\eta}\left(\mathbf{U}_{i+1,j+1,k} + \mathbf{U}_{i,j+1,k} - \mathbf{U}_{i+1,j-1,k} - \mathbf{U}_{i,j-1,k}\right),$$

$$\left.\frac{\partial \mathbf{U}}{\partial \varsigma}\right|_{i+\frac{1}{2},j,k} = \frac{1}{4h_\varsigma}\left(\mathbf{U}_{i+1,j,k+1} + \mathbf{U}_{i,j,k+1} - \mathbf{U}_{i+1,j,k-1} - \mathbf{U}_{i,j,k-1}\right)$$

Here $\mathbf{U} = \left(C_1, C_2, \ldots, C_K, u, v, w, T\right)^{\mathrm{T}}$ — vector of primitive dependent variables of the problem. In this work $K = 8$ and the total number of dependent variables is 12.
It seems that derived implicit nonlinear numerical scheme is absolutely stable for the linear problem.

2.2 Solution of nonlinear difference equations

As a result of described approximation of RANS equations and corresponding boundary conditions, integration of nonlinear partial differential equations reduces to solution of nonlinear system of algebraic equations

$$\mathbf{R}\left(\mathbf{X}\right) = 0,$$

where $\mathbf{X}$ - vector of dependent variables (node values of gas-dynamic variables, including boundary nodes). This problem is effectively solved using iterative Newton method, clear advantage of which is a quadratic convergence rate. For solution of nonlinear finite-difference equations modified Newton-Raphson is used:

$$\mathbf{X}^{[k+1]} = \mathbf{X}^{[k]} - \tau_{k+1}\mathbf{D}_{k0}^{-1}\mathbf{R}\left(\mathbf{X}^{[k]}\right)$$

where $\mathbf{D}_{k_0} = \left(\partial \mathbf{R} / \partial \mathbf{X}\right)_{k_0}$ — Jacobian matrix, k, k_0 — iteration numbers, $k_0 \le k$, $\mathbf{R}\left(\mathbf{X}^{[k]}\right)$ — residual vector. Expression $\mathbf{D}_{k0}^{-1}\mathbf{R}\left(\mathbf{X}^{[k]}\right) = \mathbf{Y}^{[k]}$ is a solution of linear system of equations $\mathbf{D}_{k_0}\mathbf{Y}^{[k]} = \mathbf{R}\left(\mathbf{X}^{[k]}\right)$. In process of numerical solution regularization parameter of Newton method relative to initial approximation τ_k is determined as follows:

$$\tau_{k+1} = \frac{\left(\mathbf{Y}^{[k]} - \mathbf{Y}^{[k-1]}, \mathbf{Y}^{[k]}\right)}{\left(\mathbf{Y}^{[k]} - \mathbf{Y}^{[k-1]}\right)^2}$$

As iterative process converges $\tau_k \to 1$, and convergence rate theoretically tends to quadratic one.

The most labor-consuming algorithm elements in Newton method realization are matrix $\mathbf{D}_{k_0} = \left(\partial \mathbf{F} / \partial \mathbf{X}\right)_{k_0}$ generation and following solution of linear system of equations with this matrix.
Since in approximation of equations at every cell only several neighbor nodes are used (in three-dimensional case 25 nodes for TVD scheme), laboriousness of Jacobian matrix generation is $O(N)$, where N — number of nodes for finite-difference problem.
RAM memory space and CPU time necessary for solution of linear system of algebraic equations on nonlinear iteration

$$\left(\partial \mathbf{R} / \partial \mathbf{X}\right)_{k_o} \mathbf{Y}^{[k]} = \mathbf{R}\left(\mathbf{X}^{[k]}\right)$$

DOI: 10.13009/EUCASS2017-281

considerably depend on matrix $\left(\partial\mathbf{R}/\partial\mathbf{X}\right)_{k_0}$ sparseness degree. When Navier-Stokes equations are approximated using second order difference scheme, operator $\left(\partial\mathbf{R}/\partial\mathbf{X}\right)_{k_0}$ has sparse block 25-diagonal structure, and its elementary block is a dense matrix (4+K) $\times$ (4+K). Preliminary calculations showed that convergence of nonlinear iterative process considerably depends on points in approximation stencil, using for convective component, and also for direct derivatives of dissipative component of Reynolds equations. Use of corner points in approximation stencil for mixed derivatives of dissipative component has weak effect on convergence of nonlinear iterations. Hereupon, and also in order to reduce RAM memory space and total number of arithmetic operations, diagonals in operator $\left(\partial\mathbf{R}/\partial\mathbf{X}\right)$, corresponding to mixed derivative are neglected. As a result, operator $\left(\partial\mathbf{R}/\partial\mathbf{X}\right)$ for three-dimensional case has block 13-diagonal structure.

Solution of linear system of algebraic equations, obtained on nonlinear iteration, is carried out with use of Generalized minimal residual algorithm *GMRes* [10], which is the most reliable and fast, according to numerical experiments [11].

The method of numerical simulation, described above, is implemented in software package HSFlow (High Speed Flow solver) with possibility of parallel calculations using multiprocessor supercomputers with distributed memory. Calculations are carried out on structured multiblock grids.

2. Simulation of flow over the segmental-conical body

One of the main goals of this work is testing of developed method and programs using calculation of flow over segmental-conical body. Geometry similar to Martian space vehicle of "ExoMars" project is used. In order to determine a descent trajectory part in Martian atmosphere with the most intensive heat transfer, calculations of flow over the body at zero angle of attack are carried out. Equilibrium radiation temperature at the front stagnation point along one possible descent trajectory is shown in Figure 1. These data correspond to absolutely catalytic relative to atomic oxygen and nitrogen surface. The maximum temperature of the space vehicle surface is reached at 40 km above Mars surface. It should be expected that at this altitude physical-chemical processes, taking place in undisturbed flow region, substantially influence heat transfer. On this account, for testing of three-dimensional flow over the space vehicle trajectory point II is used, corresponding the maximum aerodynamic heating. For comparison, results of calculations, corresponding to trajectory point I at altitude 69 km are given.

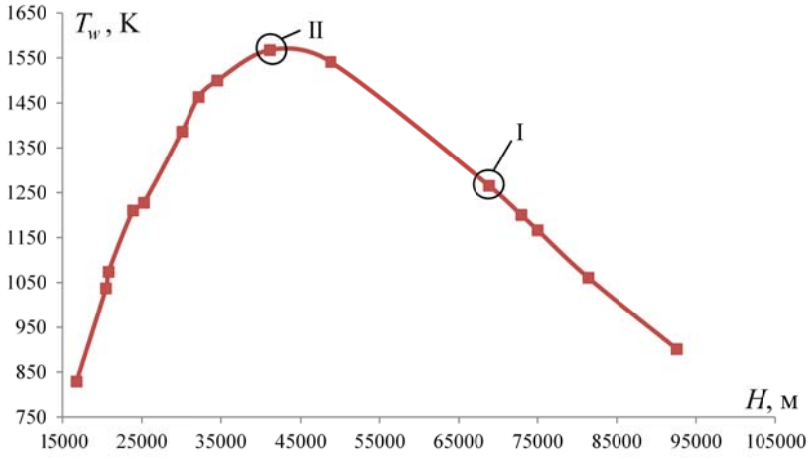

Figure 1: Temperature at stagnation point for zero angle of attack and absolutely catalytic surface

Free stream parameters, corresponding to trajectory points I and II are given in Table 2.

Table 2: Free stream parameters

DOI: 10.13009/EUCASS2017-281

No.	H, km	$\rho_\infty 10^5$, kg/m^3	p_∞, Pa	T_∞, K	$\mu_\infty 10^6$, Pa·s	M_∞	$Re_{\infty 1}$
I	69	2,4	0.734	160	8.07	29	17700
II	41	34	13.6	208	10.65	22.5	167000

Three-dimensional problem of flow over space vehicle is solved for angles of attack 0^0 and 10^0. Numerical grid is made from axisymmetric one by 180° revolution around symmetry axis (Figure 2). Numerical grid 401×201×41 (3.2 million nodes) is used, where 401 corresponds to the number of nodes along the surface, 201 – along the normal to the surface, 41 – in circular direction. Near the solid wall grid clustering is made along normal to the surface in order to resolve boundary layer. Computational grid is splitted on 48 blocks for parallel calculations using multiprocessor supercomputers.

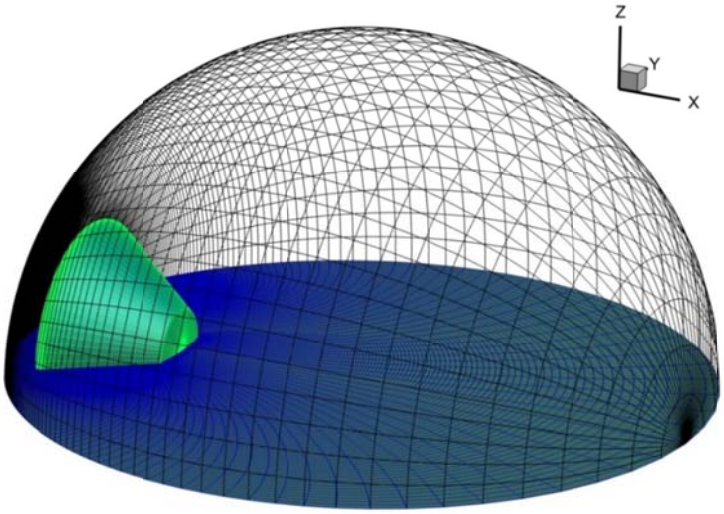

Figure 2: Surface of segmental-conical body and fragment of computational grid

The most significant characteristics, obtained in numerical simulation, are pressure distributions (Figure 3) and temperature distributions (Figure 4) along surface of flight vehicle in the symmetry plane. Higher values of pressure in Figure 3 and temperature in Figure 4 are obtained on the windward surface, lower – on the leeward surface. Integration of pressure distribution along surface allows obtaining basic forces and moments of forces, acting on the space vehicle. It is known that at hypersonic stabilization $M_\infty \gg 1$ dimensionless pressure $p_w/(\rho_\infty V_\infty^2)$ on the windward surface of flight vehicle weakly depends on Mach number and other determining parameters, and it is can be determined by Newton formula. In particular, according to data in Figure 3, dimensionless pressure virtually doesn't depend on catalytic properties of the body. One of the characteristic properties of pressure distribution on the windward surface for this body is its nonmonotonic behavior. Here regions with adverse (positive) pressure gradient can be seen. Such behavior is related to the body shape, which has curvature discontinuity in the region of spherical and conical parts conjunction. Presence of adverse pressure gradient can lead to local boundary layer separation and also to early laminar-turbulent transition on the free surface of the separation.

Aerodynamic heating of space vehicle surface during descent in Martian atmosphere is of great practical importance. Distributions of equilibrium radiation temperature of the vehicle surface in symmetry plane for catalytic and non-catalytic wall are given in Figure 4. In three-dimensional flow, for the vehicle at angle of attack, stagnation point shifts to windward surface. It is seen in Figure 4 that at angle of attack 10^0 the maximum value of temperature shifts to windward surface. It is also seen that windward part of reversed cone (in base part of the vehicle) at non-zero angle of attack experiences higher heat load, than leeward part, and temperature difference may be up to 200^o K (for point I) and 300^o K (for point II). For zero angle of attack at trajectory point I temperature increase up to 500^o K is observed.

It should be noted that catalytic properties of the surface strongly influence its heating. It can be seen from data in Figure 4 that non-catalytic surface has lower heating. In the base part this difference is not so significant, but in the front part temperature of catalytic (with respect to atomic oxygen and nitrogen) surface is 400 K greater than for non-catalytic surface. It is interesting that angle of attack 10^0 leads to substantially nonsymmetrical pressure distribution on the front surface and in flow field (Figure 5) relative to plane $y = 0$. Temperature of the front surface

DOI: 10.13009/EUCASS2017-281

has not such behavior. It is specified by chemical processes after the shock wave. Distribution analysis of mass fractions for basic species of gas mixture, shown in Figure 5, indicates higher degree of dissociation of molecule CO_2 on the windward front surface in comparison with the leeward surface. It leads to higher decrease of temperature on the windward surface in comparison with the leeward surface

a

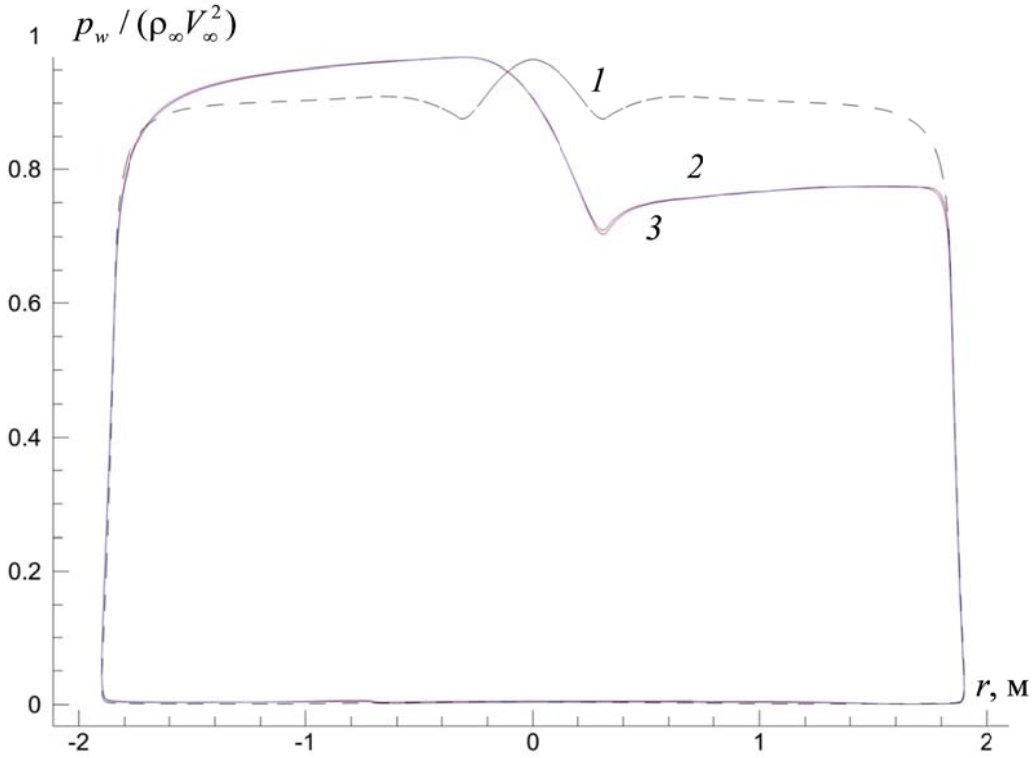

b

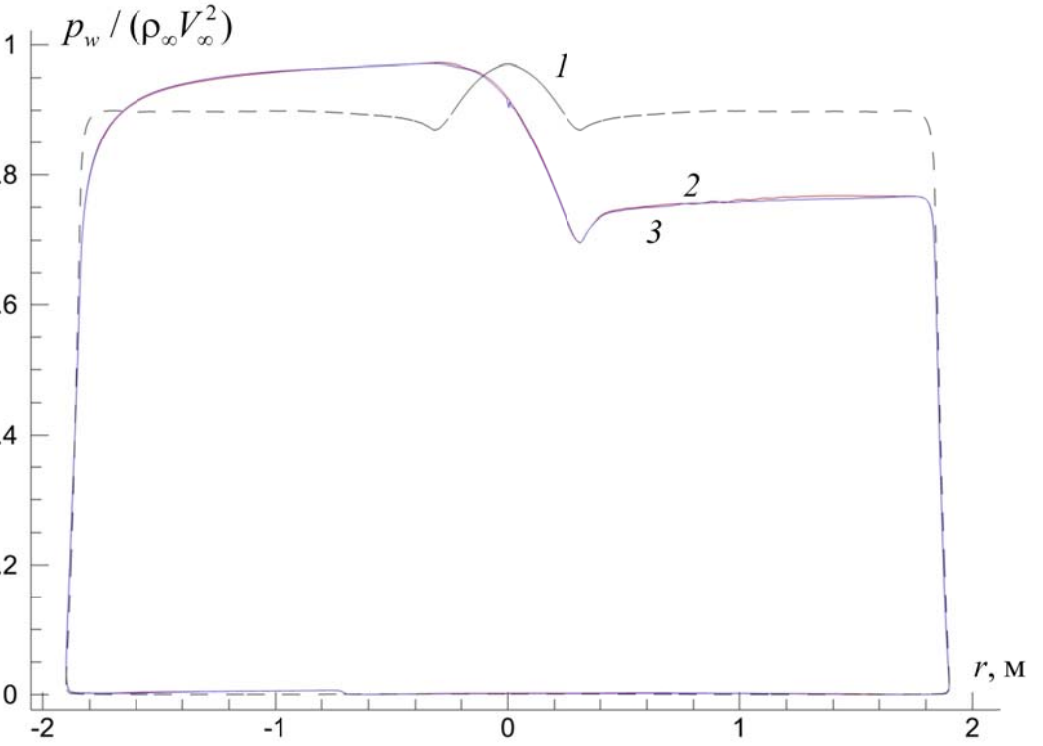

Figure 3: Pressure distribution along the surface of descent vehicle in the symmetry plane: a — point I; b — point II; 1 — catalytic surface , angle of attack 0^0; 2 — catalytic surface, angle of attack 10^0; 3 — non-catalytic surface, angle of attack 10^0, r — distance from a surface point to symmetry axis

DOI: 10.13009/EUCASS2017-281

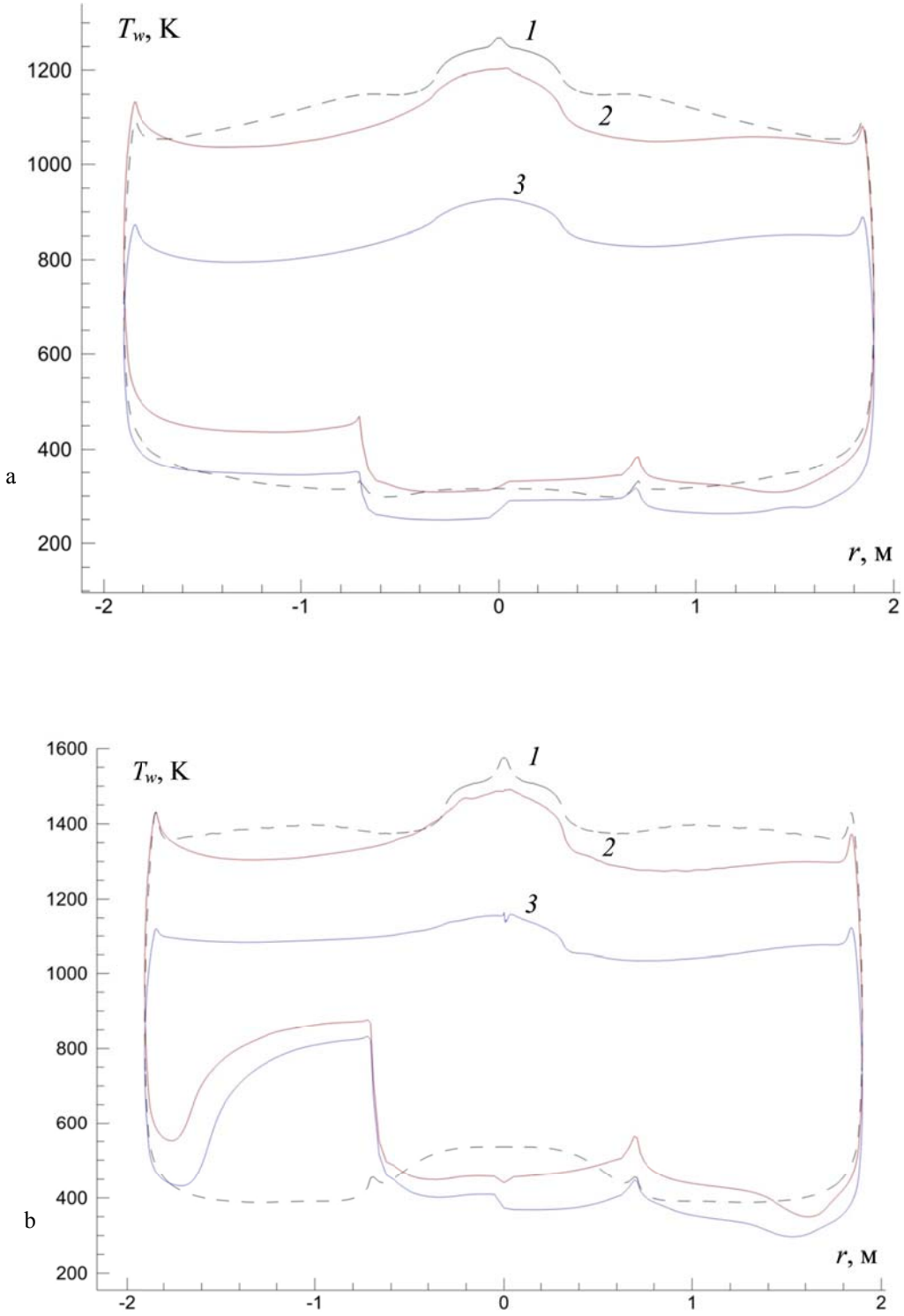

Figure 4: Temperature distribution along the surface of descent vehicle in the symmetry plane: a — point I; b — point II; 1 — catalytic surface , angle of attack 0^0; 2 — catalytic surface, angle of attack 10^0; 3 — non-catalytic surface, angle of attack 10^0, r — distance from a surface point to symmetry axis

DOI: 10.13009/EUCASS2017-281

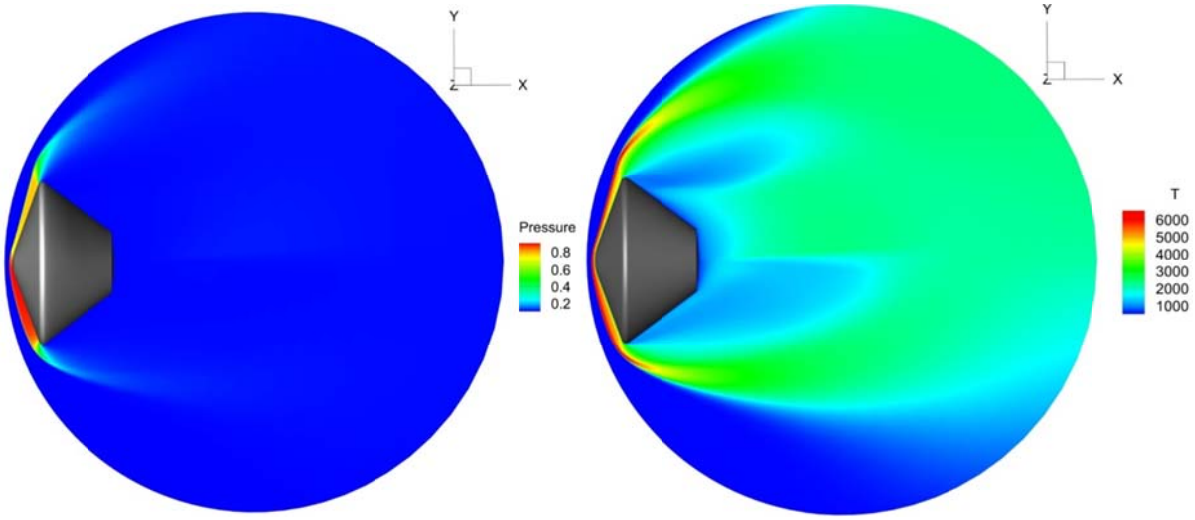

Figure 5: Dimensionless pressure and temperature fields. Trajectory point I.

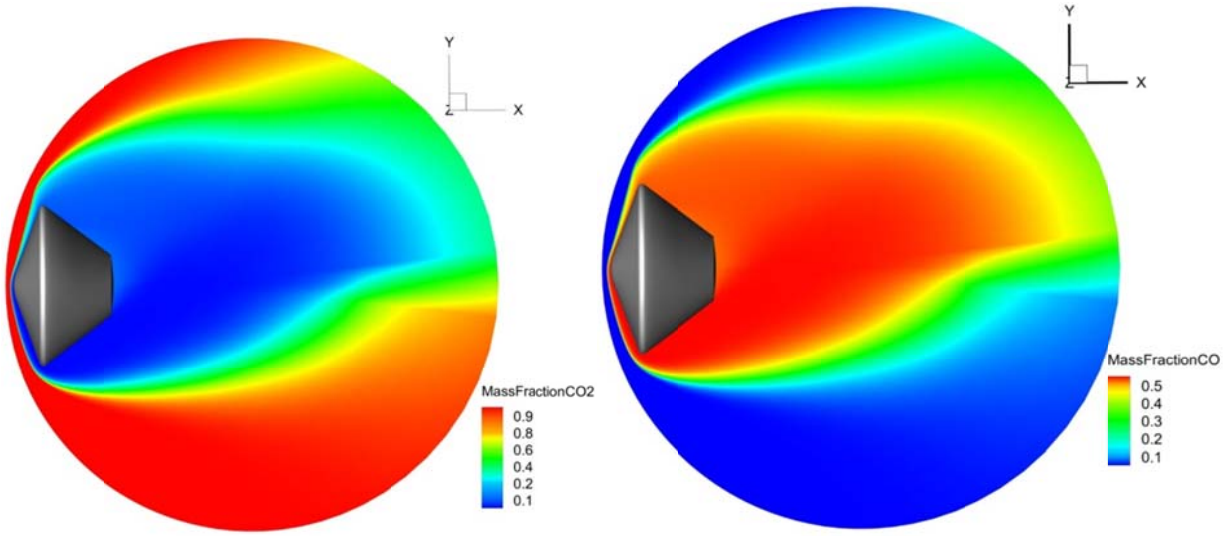

Figure 6: Fields of CO_2 and CO mass fractions. Trajectory point I.

Analysis of computational data indicates that at both trajectory points chemical reactions are rather intensive both after shock wave and in the wake behind the vehicle, where almost 80% of initial carbon dioxide dissociates into CO and O. Flow fields are substantially nonsymmetrical.
At point I gas behind the shock wave is strongly heated (up to 10000 K), but it occurs in thin layer, on the average front part behind the shock wave is heated up to 5000 K. At point II velocity of the vehicle decreases, and gas temperature in the front region is significantly lower (approximately 1000 K lower), and on the average it is heated up to 4000 K. However, at point II higher aerodynamic heating of the vehicle surface is observed (Figure 4). This is a result of atmospheric density increase with altitude decrease. At altitude 41 km it is 11 times greater, than at altitude 69 km, which leads to more intensive convective heat transfer. In addition it should be noted that at point I gas in the wake behind the vehicle is also strongly heated (approximately to 3000 K), and at point II wake temperature is not greater than 2000 K. It is induced by lower velocity at this trajectory point.

3. Conclusions

Method of numerical solution of Navier-Stokes equations with non-equilibrium physical-chemical processes in Martian atmosphere is developed. The problem solution is carried out with help of original software package HSFlow with effective parallel algorithm for supercomputers.

DOI: 10.13009/EUCASS2017-281

Testing of software package HSFlow is fulfilled using problem of three-dimensional hypersonic flow over segmental-conical body, having shape similar to Martian space vehicle “ExoMars”.
Results of test calculations show that in three-dimensional flow over space vehicle at angle of attack 10^0 surface heating is rather less, than in axisymmetric flow. Windward surface of the reversed cone (in base part of the vehicle) experiences higher heat loads, than leeward surface, and temperature difference is about 300 K for trajectory point II.
It is also shown than catalytic property of a surface strongly influences the vehicle heating. For both trajectory points, the front surface temperature for catalytic surface is 400 K higher, than for non-catalytic.
Pressure distribution becomes sufficiently nonsymmetrical with angle of attack change, and pressure on the windward part is 1.3 higher, than on leeward. Temperature distribution is uniform along the front surface. This is specified by physical-chemical processes.
At both trajectory points chemical reactions are rather intensive both behind the shock wave and in the wake behind the vehicle, where nearly 80% of initial carbon dioxide dissociates into CO and O.
The reported study was funded by the Russian Science Foundation (project no. 14-19-00821-П).

References

[1] Gorelov V.A., Gladyshev M.K., Kireev A.Y., Yegorov I.V., Plastinin Y.A., and Karabadzhak G.F. 1998. Experimental and Numerical Study of Nonequilibrium Ultraviolet NO and N2+ Emission in Shock Layer. *Journal of Thermophysics and Heat Transfer*. 12:172-179.
[2] Egorov I.V., Novikov A.V., and Palchekovskaya N.V. 2017. Peculiarities of supersonic flow over segmental-conical bodies. *Computational mathematics and mathematical physics* (accepted for publication).
[3] Gupta R.N., Yos J.M., Thompson R.A., and Kam-Pui Lee. 1990. A review of reaction rates and thermodynamic and transport properties for an 11-species air model for chemical and thermal nonequilibrium calculations to 30000 K . *NASA Reference Publication* No. 1232.
[4] Godunov, S. K. 1959. A difference method for numerical calculation of discontinuous solutions of the equations of hydrodynamics. *Mat. Sb.* (*N.S.*). 47:271–306.
[5] Godunov, S. K., Zabrodin, A. V., Ivanov, M. Ya., Kraiko, A. N., and Prokopov, G. P. 1976. Computational solution of multidimension problem of gasdynamic. Moscow: Nauka.
[6] Roe, P. L. 1981. Approximate Riemann solvers, parameter vectors, and difference schemes. *J. Comp. Phys*, 43:357 – 372.
[7] Kolgan, V. P. 1972. Application of principle minimal values of derivative for construction finite-difference schemes for calculation of discontinuous solutions of gas-dynamic. *Uch. Zap. TsAGI*. 6:68–77.
[8] Harten, A. 1983. High resolution schemes for hyperbolic conservation laws. *J. Comput. Phys*. 49: 357.
[9] Ivanov, M. Ya., Krupa, V. G., and Nigmatullin, R. Z. 1989. A high-accuracy version of Godunov's implicit scheme for integrating the Navier–Stokes equations. *USSR Computational Mathematics and Mathematical Physics*. 29:170–179.
[10] Saad, Y., and Shultz, M.H. GMRes: a generalized minimal residual algorithm for solving non symmetric linear systems. *SIAM J. Scient. and Statist.Comp*. 7:856–869.
[11] Babaev, I. Yu., Bashkin, V. A., and Yegorov, I. V. 1994. Numerical solution of the Navier-Stokes equations using variational iteration methods. *Computational Mathematics and Mathematical Physics*. 34:1455–1462.